

Supplementary data to:

Hepatic Arterial Infusion of Low-Density Lipoprotein Docosahexaenoic Acid
Nanoparticles Selectively Disrupts Redox Balance in Hepatoma cells and Reduces
Growth of Orthotopic Liver Tumors in Rats

Xiaodong Wen¹, Lacy Reynolds¹, Rohit S. Mulik¹, Soo Young Kim¹, Tim Van Treuren¹,
Liem H. Nguyen^{2,3}, Hao Zhu^{2,3} and Ian R. Corbin^{1,3*}

¹Advanced Imaging Research Center, ²Children's Research Institute Department of Pediatrics, ³Internal Medicine Division of Liver and Digestive Diseases, University of Texas Southwestern Medical Center at Dallas, Dallas, TX 75390, USA

Table of Contents

Supplementary Materials and Methods.....	4
Cell Culture and Animals.....	4
Hepatocyte isolation.....	4
Mouse and human cell lines.....	4
Orthotopic HCC implantation.....	5
Hepatic arterial injection.....	5
Tumor size determination by MRI.....	6
Fluorescent LDL tracking studies.....	7

Preparation of LDL-DiR nanoparticles.....	7
Biodistribution study.....	7
Optical fluorescence imaging.....	8
Fluorescence microscopy.....	8
MYC-induced HCC mouse model.....	8
Serum analysis.....	9
Pathology.....	9
Cell toxicity assay (MTS).....	10
Cell death assay.....	10
Lipid peroxidation.....	10
Measurements of oxidative stress.....	10
Cellular reactive oxygen species.....	11
Detection and quantitation of protein carbonyls.....	11
Measurements of NADPH/NADP.....	12
Measurement of total GSH (GSH + GSSG), GSSG and GSH/GSSG ratio.....	12
Redox potential.....	13
Western Blot and immunohistochemistry.....	13
Immunoblot.....	13

Immunohistochemistry.....13

Supplementary Figures.....14

Supplementary References.....33

ACCEPTED MANUSCRIPT

Supplementary Materials and Methods

Experimental Procedures

Cell Culture and Animals

Hepatocyte isolation

Hepatocytes were isolated from ACI rats by non-recirculating collagenase perfusion through the inferior vena cava. Livers were perfused *in situ* with 120 ml Gibco Liver Perfusion Media (Invitrogen, Carlsbad, CA) followed by 120 ml of Gibco Liver Digestion Media (Invitrogen). Thereafter, the livers were excised, their capsules removed and the liver cells were liberated. The liver cell suspension was then filtered with a Falcon cell strainer (70 μ m; Becton Dickinson, Bedford, MA), washed twice with 40 ml of Hepatocyte wash media (Invitrogen) along with centrifugation at 50 x g for 4 min. The viability of the isolated hepatocytes, as determined by the exclusion of trypan blue, was > 85%. Hepatocytes were plated on collagen coated plates/dishes in Weymouth supplemented with 5% FBS, 10 mM nicotinamide, 20 ng/ml EGF, 1x insulin, transferrin, selenium, 10^{-7} M dexamethasone, 1 % DMSO and 1x antibiotic/antimycotic. The hepatocytes were cultured at 37°C with 5% CO₂ and the media was changed every other day. These culture conditions allow the cells to maintain their proliferative capacity and differentiated functions of mature hepatocytes.¹

Mouse and human cell lines

The murine (Hepa1C7 and TIB-75) and human (SK-Hep1) HCC cell lines were obtained from ATCC (Manassas, VA) and cultured in DMEM supplemented with 10% FBS (Invitrogen, Carlsbad, CA). Primary mouse hepatocytes were isolated from Balb/C mice using a non-recirculating collagenase perfusion as described earlier for the rat. Lastly, the immortalized non-malignant human hepatocyte cell line, Thle2 was also purchased from ATCC and cultured

according to the manufacturers recommendations. All cells were grown at 37 °C in a 5% CO₂ atmosphere in a humidified incubator.

Orthotopic HCC implantation

H4IIE cells grown in culture were subsequently inoculated directly into the liver parenchyma of 24 male ACI rats. Animals were anesthetized with isoflurane (2.5%) in air for the inoculation procedure. Briefly, the surface of the rat's abdomen was aseptically cleaned with Betadine and a subcostal midventral incision made to expose the left lobe of the liver. The left lobe was directly injected with 1×10^6 H4IIE cells using a 30 gauge needle, pressure was applied to the injection site with a sterile cotton tip applicator until hemostasis was attained. The left lobe of the liver was returned to the abdominal cavity and the incision was closed in two layers with absorbable sutures. Buprenex (0.05-0.1 mg/kg) was administered (intraperitoneal) to the rats in the post-operative period.

Hepatic arterial Injection

Briefly, tumor bearing rats were anesthetized with isoflurane and a midline laparotomy was performed to expose the hepatic and gastroduodenal arteries. The latter was cannulated with a PE10 polyethylene catheter using a dissecting microscope and the catheter was advanced, in a retrograde fashion, to the hepatic artery. The LDL nanoparticle solution was injected slowly, typically 1 minute for 0.3 mL suspension. Following the injection the gastroduodenal artery was ligated and careful inspection of the surgical area was done to ensure that there was no bleeding and that normal hepatic circulation was restored. The abdominal cavity and the incision were closed in two layers with absorbable sutures and the animal was allowed to recover.

Tumor size determination by MRI

Ten to fourteen days post tumor cell inoculation animals were assessed for liver tumors using MRI. The imaging examinations were performed on a 4.7 T Varian Inova imaging system equipped with a 40 cm horizontal bore magnet. Anesthesia were provided using 1% Isoflurane and a fiber optical temperature probe and pneumatic pillow (SA Inc., Stony Brook, NY) was used to monitor/regulate core temperature and respiration. Next animals were placed prone in a 60 mm diameter $^1\text{H}/^{13}\text{C}$ rat volume coil (Doty Scientific, Inc., Columbia, SC) and placed inside the magnet for proton imaging. Animals were fully monitored and warm air will be blown over the animal during the scan. Fast spin-echo multislice T2 weighted images were acquired in the sagittal and axial planes with a repetition time (TR) = 2500 ms, echo time ($\text{TE}_{\text{effective}}$) = 60 ms, slice thickness of 2 mm, field of view (FOV) 80 mm x 40 mm (sagittal), 60 mm x 60 mm (axial) and a matrix size of 512 x 256 (sagittal), 256 x 256 (axial). Animals will be allowed to recover after the MRI session and returned to their cages. The sagittal and axial images were used to measure tumor size before treatment and for evaluating therapy response after treatment. The formula used to compute tumor volume was based on the standard volume of an ellipsoid, as follows:

$$V=4/3\pi(x.y.z)$$

where x,y , and z are the three radii (half diameters) measurements of the tumor. Measurement of the longest diameter and the longest perpendicular diameter of tumor was carried out for each image. The measurement for the third diameter was estimated based on the presence of the tumor in serial image slices and the slice thickness of each image. Measurements from both the sagittal and axial images ensured accurate measures of tumor diameters in all three x,y and z planes. Measurements of the tumor dimensions were carried out using ImageJ software (NIH; <http://rsb.info.nih.gov/ij>; version 1.30).

Fluorescent LDL Tracking Studies

Preparation of LDL-DiR nanoparticles

Fluorescent labelled LDL was prepared by incubating the lipophilic carbocyanine dye DiR (1,1'-Dioctadecyl-3,3,3',3'-Tetramethylindotricarbocyanine Iodide) with LDL at a molar ratio of 82:1. The reaction was carried out at 37°C for 18 h, followed by removal of excess label using ultracentrifugation (49,000 rpm for 20 h at 4°C).² These reaction conditions typically result in a DiR fluorophore-to-protein ratio of ~5:1 and a protein recovery higher than 60%.

Biodistribution Study: DiR Fluorescence Measurement

A biodistribution study was performed to evaluate the distribution of the LDL-DiR nanoparticles throughout the body following HAI (5 nM). Four hours post injection blood was collected via cardiac puncture and the animals (n=4) were euthanized. Organs and tumor were excised and collected for subsequent imaging and biodistribution analyses. Accurately weighted tissue sections were collected in glass tubes containing 1 mL phosphate buffer saline (PBS, pH 7.4). Tissues samples were homogenized using a high speed homogenizer to produce a homogenous slurry. To this slurry, 2 mL of chloroform:methanol mixture (2:1) was added and vortexed thoroughly for 20 seconds. All the samples were then centrifuged at 2000 rpm for 10 min, and the chloroform layer containing DiR was collected, dried under a stream of nitrogen and re-dissolved in 1 mL chloroform. The DiR fluorescence was measured using fluorescence spectrometry (Hitachi F-7000 Fluorescence Spectrophotometer, Hitachi, CA, USA) at excitation and emission wavelengths of 710 nm and 780 nm respectively. The concentration of DiR was determined using a standard curve of DiR obtained using the same method.

Optical Fluorescence Imaging: Xenogen IVIS System

Fluorescence imaging of the excised liver and tumor was performed using Xenogen IVIS optical imaging system. Tissue samples were imaged for the detection of DiR fluorescence using excitation and emission wavelengths of 710 nm and 780 nm respectively.

Fluorescent Microscopy

Liver and tumor cryo-tissue sections prepared from control animals and animals injected with LDL-DiR nanoparticles were mounted in ProLong Gold mounting medium containing DAPI nuclear counterstain (Invitrogen). The slides were scanned using a Zeiss Axioscan.Z1 microscope at 20X magnification using excitation and emission filter sets appropriate to detect DAPI and near-infrared signals. Exposure times were held constant for control and experimental slides (20ms for DAPI and 1sec for DiR). Digital images were processed including adjustment of brightness and contrast of the complete images using Zeiss Zen Lite software.

MYC-induced mouse model of HCC

Mice with *MYC*-driven liver tumors served as an additional animal model to assess the anticancer effects of LDL-DHA. The *MYC*-driven liver tumors were generated in mice by crossing the TRE-*MYC* strain with LAP-tTA mice (described previously by Beer et al. 2004).³ Offspring mice possessing both trans genes were maintained on 1mg/ml of doxycycline to conditionally suppress *MYC* expression and tumorigenesis. In the present study, doxycycline was removed for *MYC* activation at birth (neonate). These mice typically exhibit progressive abdominal enlargement during their second to third weeks of life as a result of aggressive tumor growth and hepatomegaly. On average the *MYC* overexpressing mice succumb to their liver cancer within 8 weeks.³ The anticancer effects of LDL-DHA nanoparticles were evaluated in

the *MYC* tumor bearing mice starting at day 40. HAI could not be performed in mice, as a result of their small anatomy; instead mice were randomly allocated to receive three intravenous treatments of either LDL-TO (n=7) or LDL-DHA (n=7) nanoparticles. The LDL nanoparticles were administered via the tail vein every other day at a dose of 4mg/kg. Twenty four hours after the last dose abdominal girth measurements were performed and the animals were euthanized. Liver and tumor tissue were collected for subsequent measures of lipid peroxidation (TBARS) and tumor cell proliferation (phosphor-H3)⁴.

Serum Analysis

Serum was isolated from collected blood samples and a panel of conventional liver function tests was performed on a Vitros 250 chemistry analyzer (Ortho-Clinical Diagnostics). Plasma chemistry tests included: blood urea nitrogen (BUN); creatinine (CREA); albumin (ALB); aminotransferase (AST), alanine aminotransferase (ALT); alkaline phosphatase (ALKP); total bilirubin (TBIL); and gamma glutamyltransferase (GGT).

Pathology

At the time of euthanasia, samples of liver, tumor and spleen were collected, fixed in 10% formalin and paraffin embedded. Five-micrometer thin sections were subject to either hematoxylin-eosin (HE) staining for histological analysis or no staining for immunohistochemistry (see below). HE tumor tissue sections were graded by a blinded histopathologist for inflammation and necrosis. Inflammation was graded on a scale from 0-3 where: 0= absent; 1= minimally affected; 2= mildly affected; 3= moderately affected. Similarly, necrosis was graded from 0-3 as follows: 0=absent; 1= 0-33% necrotic; 2= 34%-66% necrotic; 3= 67%-100% necrotic.

Cell toxicity assay (MTS)

Each cell type was seeded in 96-well plates (7×10^3 H4IIE cells/well and 35×10^3 hepatocytes /well). After 72 hours of culture, the cells received various concentrations of the LDL-DHA nanoparticles ranging from 0 to 100 μM (DHA). For controls (LDL-TO/ LDL-OA), dosing went as high as 200 μM . At the end of the 72 hour treatment period, the cell viability was measured by the MTS assay as recommended by the manufacturer. In brief, 100 μL MTS solution was added to each well and cells were incubated at 37°C for 4 hours followed by absorbance readings at 450 nm. The relative cell viability is expressed as a percentage of the non-treated controls.

Cell death assay

Seventy-two hours following LDL nanoparticle treatments (40 μM) (as described above), cells were stained with the Promokine Apoptotic/Necrotic Cells Detection Kit according to the manufacturer's protocols. The annexin-V FITC and propidium iodide (PI) double staining method was used to provide readouts of apoptotic and necrotic cells, respectively. Cells were analyzed with a Leica TCS SP5 confocal microscope (Leica Microsystems Inc., Buffalo Grove, IL).

Measurements of Oxidative Stress**Lipid peroxidation**

The total amount of lipid peroxidation products formed in the cells was determined using the thiobarbituric acid (TBA) method⁵.

Cellular reactive oxygen species

Cellular reactive oxygen species (ROS) content was measured by incubating cells with 10 μ M dihydroethidium (DHE) (Invitrogen) for 30 minutes at 37°C. After incubation, cells were washed with PBS, centrifuged (66 x g for 5 min) and resuspended in 1 ml of acetonitrile. The samples were then sonicated intermittently (amplitude 10) for 20 sec intervals on ice, cell debris was pelleted by centrifugation (9,000 x g for 15 minutes at 4°C) and the acetonitrile supernatant was collected for fluorescence spectrophotometry. The remaining cell pellet was resuspended in 1 ml PBS and later used for protein determination. Fluorescence measurements were acquired on a Hitachi F-7000 fluorescence spectrophotometer with excitation at 490 nm and an emission scan from 520-650 nm. Fluorescence reading were recorded as a fold change of fluorescence intensity units at 570 nm per mg of cell protein with respect to the untreated controls.

In situ reactive oxygen species (ROS) production was also evaluated by staining with DHE. Collected tissues were immediately submerged in OCT solution and frozen in isopentane cooled by liquid nitrogen. Thereafter frozen tissue blocks were stored at -80 °C until cyrosectioning. Unfixed frozen tissue sections (10 μ m) were later incubated with 2 μ M DHE (diluted in acetone from 1 M stock solution in DMSO) at 37 °C for 30 min in a humidified chamber. Excess stain was removed by blotting slide on filter paper. Fluorescence was detected with an upright fluorescent microscope using the TX red filter set at 10x and 20x magnification.

Detection and Quantitation of Protein Carbonyls

Quantitation of protein-bound carbonyl as 2,4-Dinitrophenylhydrazine (DNPH) derivatives was performed by incubating an aliquot of the cell suspension (0.5 mL, 0.5×10^6 cells) or tissue extract with an equivalent volume (0.5 mL) of 0.1% DNPH in 2.0 N HCl (w/v) for 1 hour at room temperature. This reaction was terminated and total cellular protein precipitated by the addition of an equivalent volume (1.0 mL) of 20% TCA (w/v). Cellular protein was rapidly pelleted by

centrifugation at 9000 x g, and the supernatant was removed. Excess unreacted DNPH was extracted three times with an excess volume (0.5 mL) of ethyl acetate:ethanol (1:1, v/v). Following the extraction, the recovered cellular protein was dried under a nitrogen stream and solubilized in a solution (1.0 mL) of Tris-buffered 8.0 M guanidine-HCl, pH 7.2. Protein-bound DNPH was detected using a UV spectrophotometer operating between 190 and 400 nm, where the maximum absorption of protein-bound carbonyls occurs at 366–370 nm. The sample protein-bound carbonyl readings were normalized to total protein content.

Measurement of NADPH/ NADP

NADPH/NADP concentrations in cell and tissue samples were determined by using EnzyChrom NADPH/NADP assay kit (BioAssay Systems). The kit is based on a glucose dehydrogenase cycling reaction, in which a tetrazolium dye (MTT) is reduced by NADPH in the presence of phenazine methosulfate. The intensity of the reduced product color measured at 565 nm is proportionate to the NADPH/NADP concentration in the sample.

Measurement of total GSH (GSH+GSSG), GSSG and GSH/GSSG ratio

Total soluble GSH and GSSG were measured in cell lysates/ tissue homogenate using the enzymatic recycling method.⁶ Briefly, about 3×10^6 cells or 40 mg of tissue were homogenized in 10 volumes of cold sulfosalicylic acid (0.6%) plus 0.1% Triton-X (for cells) or 5% metaphosphoric acid (tissues). Protein was precipitated and the supernatant was used to determine reduced glutathione (GSH) and glutathione disulphide (GSSG). Total glutathione (GSH + GSSG) was determined by spectrometry by measuring the conversion of 5, 5-dithiobis (2- nitrobenzene acid) (DTNB) to the yellow derivative 5'-thio-2-nitrobenzoic acid (TNB), measurable at 412 nm, in the presence of NADPH and GSH reductase. GSSG determination was similar for total glutathione, except that GSH was first derivatized for 1 h with 2-vinylpyridin. Change in absorbance at 412 nm was recorded for 3 min. The GSH level was calculated by

subtracting GSSG content from the total glutathione content ($GSH = \text{total GSH} - 2GSSG$). Results were expressed in mmol per mg of cell protein and mmol per gram of weight for the tissues.

Redox potential

The redox potential of the glutathione redox couple was quantified by the Nernst equation ($E_{hc} = E_0 + 30 \log ([GSSG]/[GSH]^2)$, wherein E_0 is taken as -264 mV at pH 7.4.⁷ The Nernst potential was calculated from the experimentally determined molar concentration of GSH and GSSG in cell and tissue samples. The Nernst potential takes into account not only the GSH/GSSG ratio but also the absolute concentration of GSH, where any changes in the latter will change the redox potential even without significant changes in the GSH/GSSG ratio.

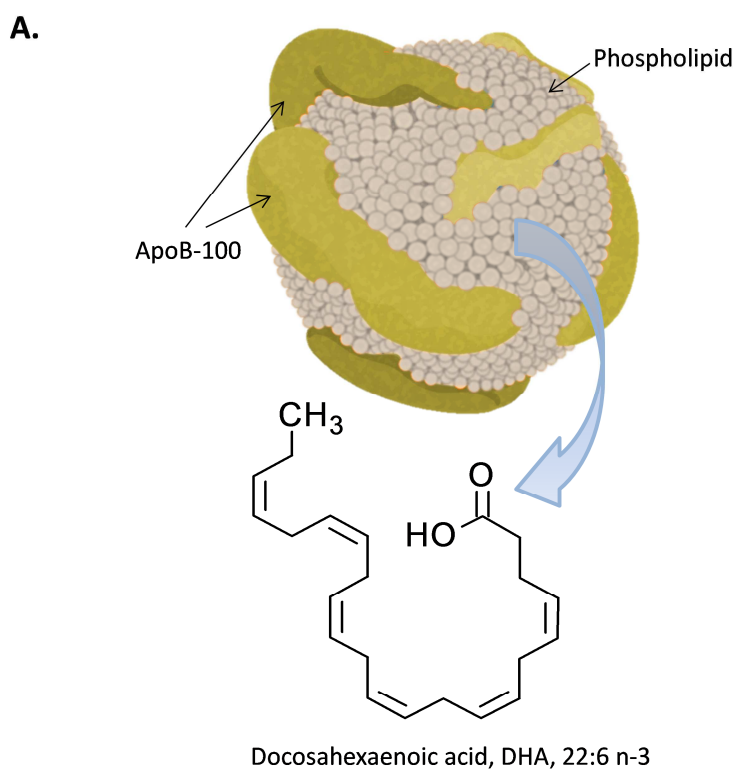
Western Blot and Immunohistochemistry

Immunoblot

Cell and tissue proteins were separated on a 10% sodium dodecyl sulfate polyacrylamide gel and transferred to PVDF. Membranes were then probed with antibodies from Santa Cruz against superoxide dismutase 1 (SOD-1 ((FL-154) sc-11407), catalase ((N-17) sc-34280), glutathione peroxidase 4 (GPx-4 (H-90) sc-50497), and β -actin ((C4) sc-47778).

Immunohistochemistry

Immunohistochemistry was done as described previously using microwave antigen retrieval and mouse monoclonal antibody to Ki-67 (1:100 dilution; Abcam, Cambridge, MA) and cleaved caspase-3 (1:50 dilution; Abcam, Cambridge, MA). Sections treated with serum from primary antibody host animal alone served as negative controls.



B.

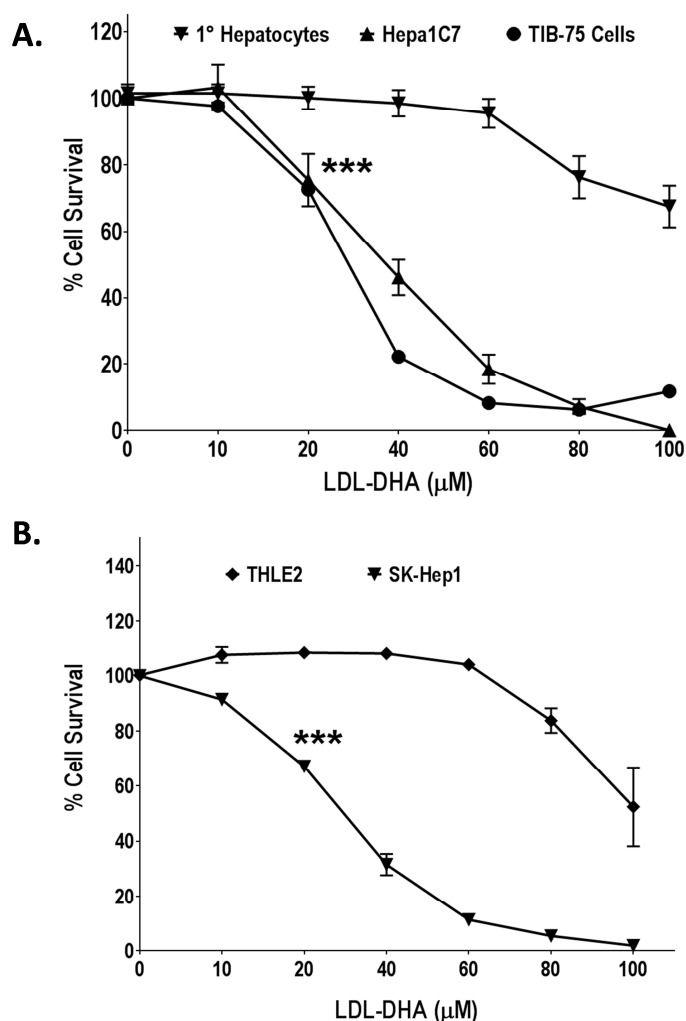
Parameter	Native LDL	LDL-TO	LDL-OA	LDL-DHA
ApoB-100 [‡]	1	1	1	1
Phospholipid [‡]	651.8 ± 140.4	652.2 ± 160.9	400 ± 29.6	541.6 ± 153.1
Cholesterol [‡]	2958 ± 378*	nd	nd	nd
Lipid cargo [‡]	**	344 ± 26.6	1350.4 ± 89.4	1152.4 ± 89.4
Diameter (nm)	18.03 ± 0.4	23.16 ± 0.4	23.7 ± 0.6	20.5 ± 1.3
Surface Charge (mV)	-9.0 ± 0.9	-14.8 ± 0.6	-25.0 ± 0.4	-25.0 ± 1.6

[‡] Values are expressed in number of molecules per LDL particle.

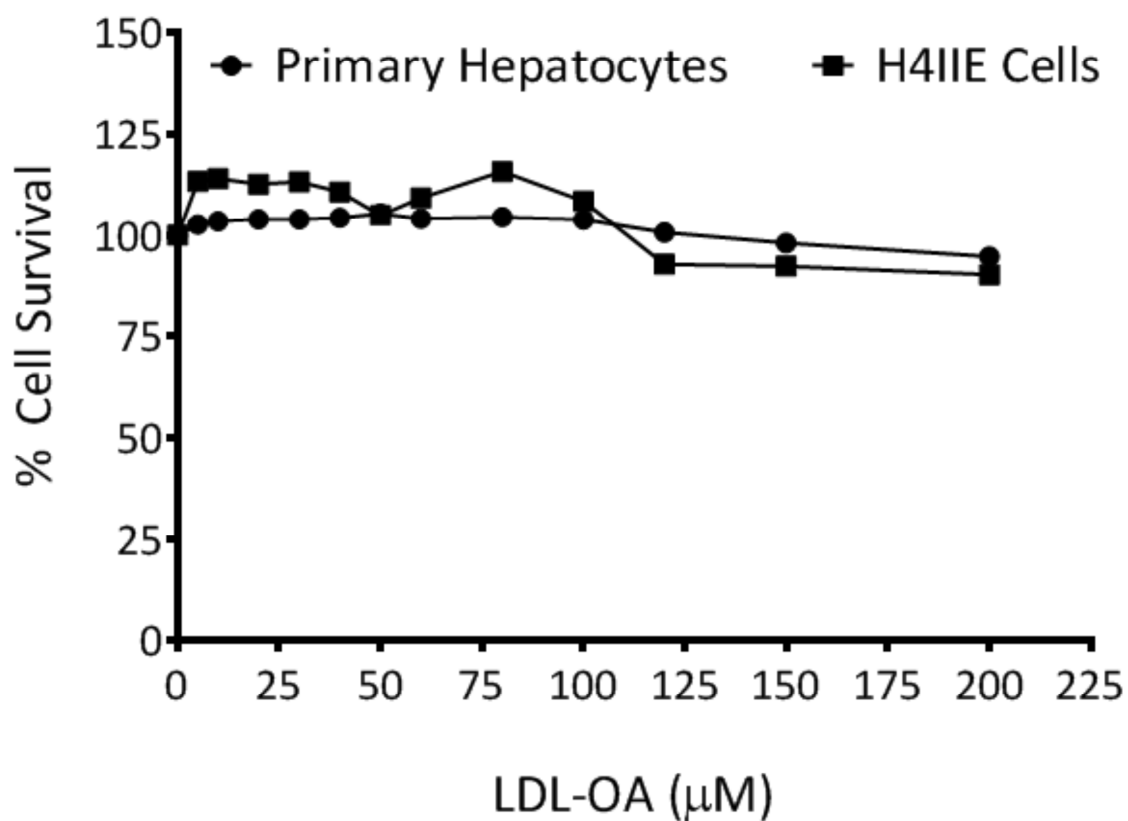
*Total cholesterol includes cholesteryl esters and free cholesterol. Literature values indicate that LDL typically carries between 1300-1600 cholesteryl esters and 500-600 free cholesterol molecules

** LDL also carries about 170 triglyceride molecules. DHA typically makes up only 1% of the total fatty acid composition of LDL

Supplementary Figure 1. The LDL-DHA nanoparticle. (A) Schematic drawing of LDL-DHA nanoparticle. **(B)** Composition and physicochemical properties of native LDL and LDL nanoparticles.

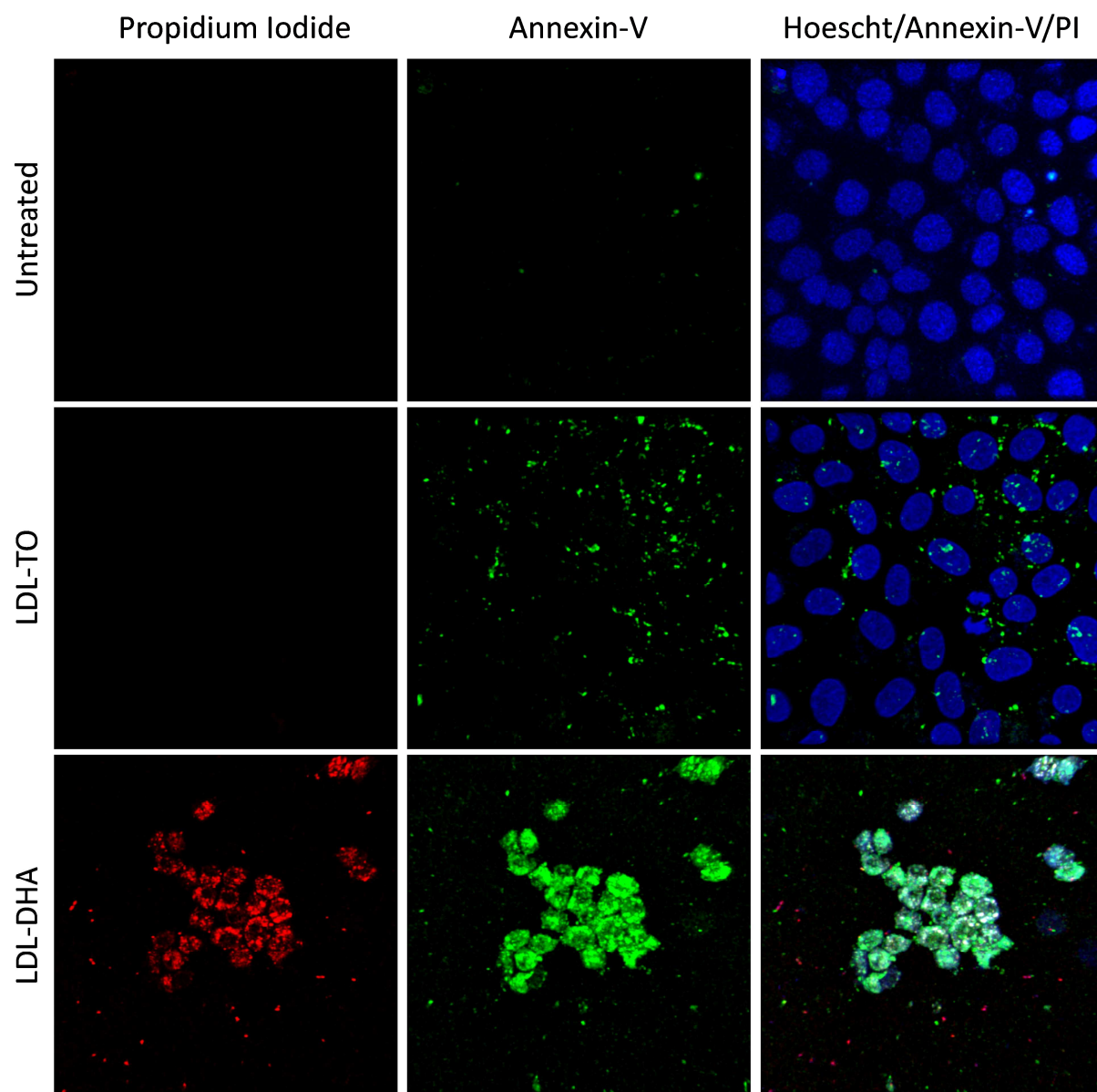


Supplementary Figure 2. Dose response of LDL-DHA in mouse and human liver cells. (A) Mouse HCC cell lines (Hepa1C7 and TIB-75) versus primary Balb/C mouse hepatocytes. **(B)** Human SK-HEP1 HCC cells versus THLE2 (a SV40 large T antigen immortalized non-malignant liver cell line). All cells were treated for 72 hours with varying doses of LDL-DHA (0-100 μM). Cell viability was determined by MTS assay normalized to untreated controls cells. Experiments were performed in triplicate wells with three independent runs. Data are expressed as mean \pm SEM. ***, $P \leq 0.001$ versus corresponding non-malignant cells. All readings after 20 μM are significant at $P \leq 0.001$ for the HCC cells.

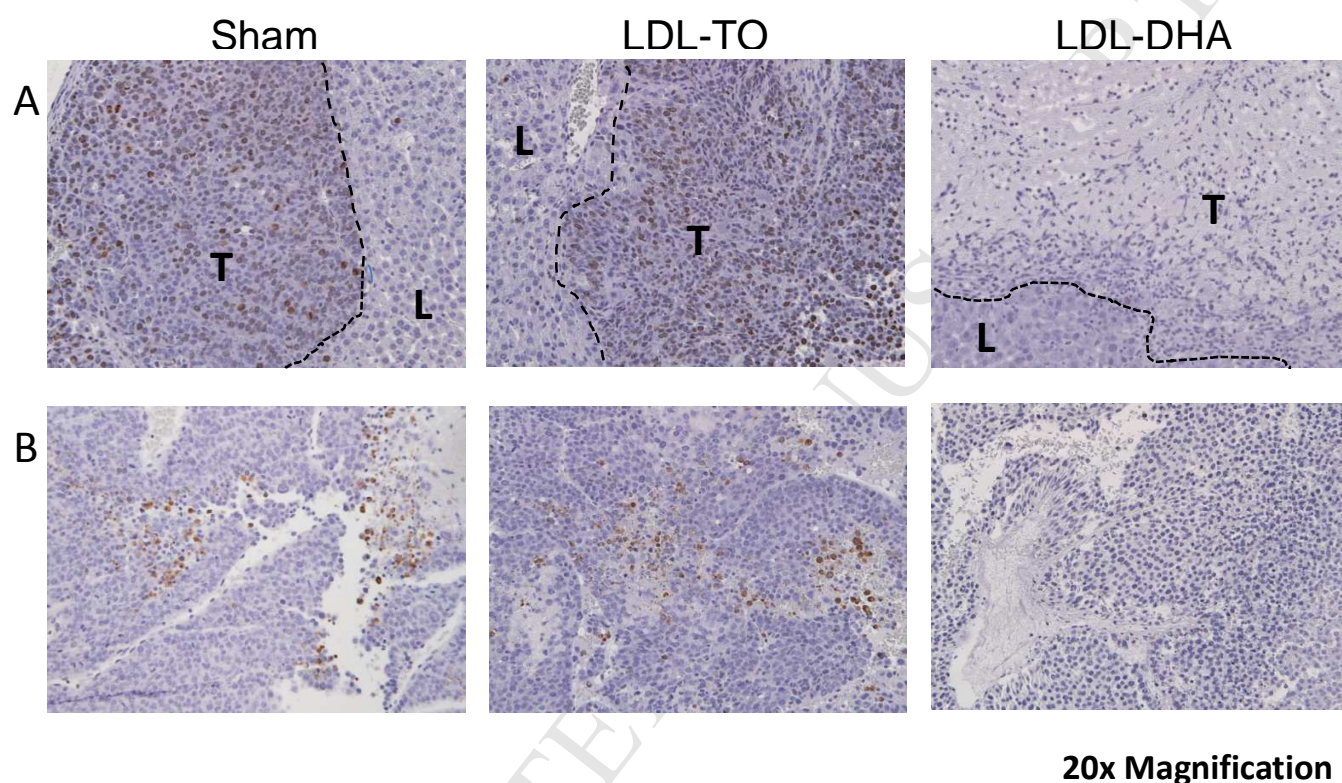


Supplementary Figure 3. Dose response of LDL-OA in H4IIE and primary hepatocytes.

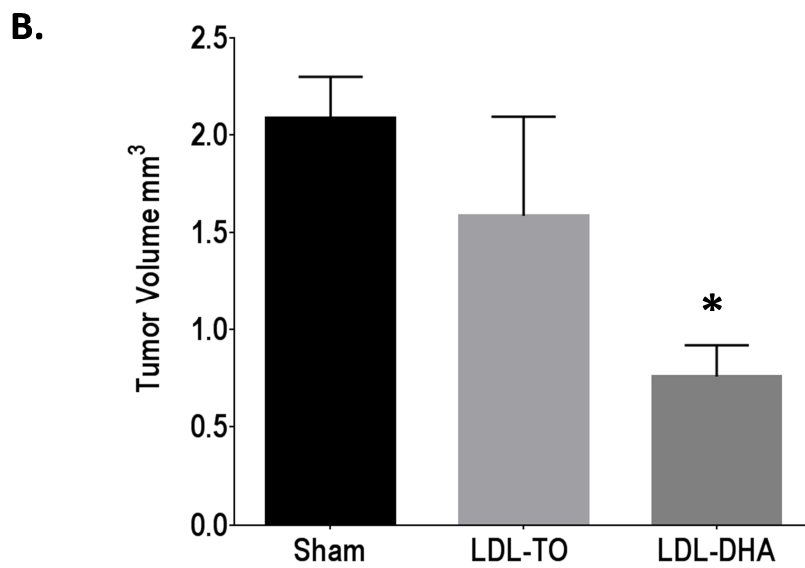
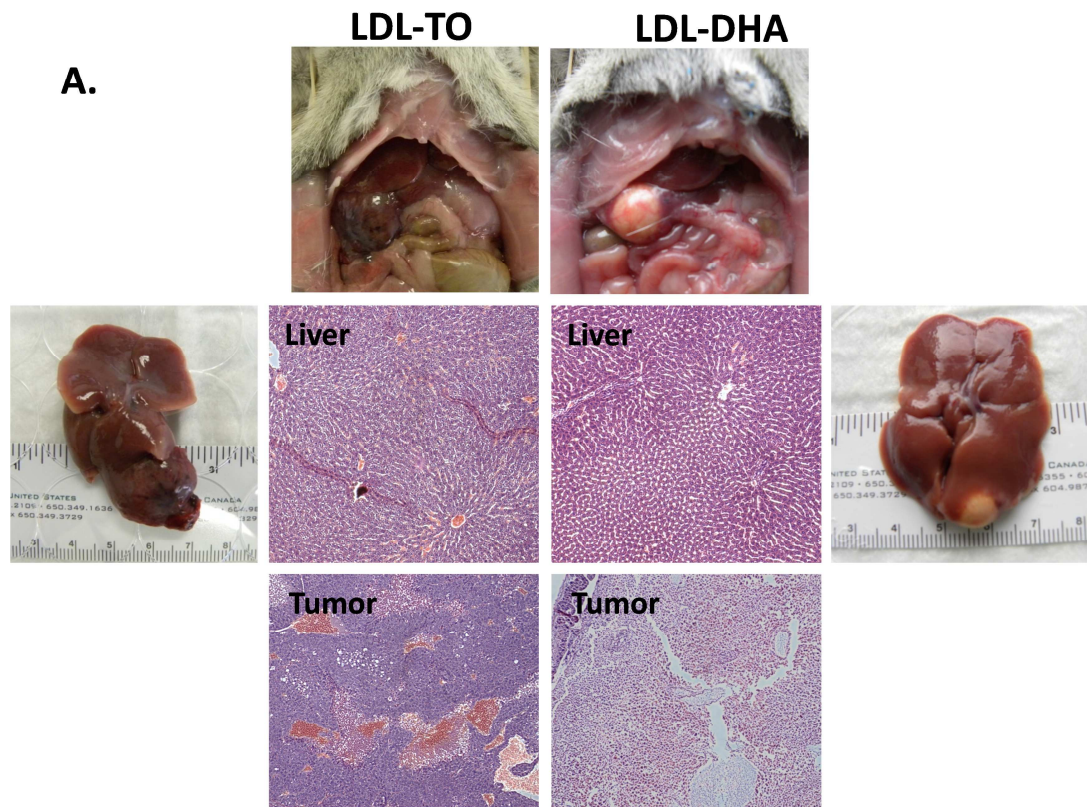
H4IIE rat HCC cells and primary hepatocytes were plated to 85% confluency and treated for 72 hours with varying doses of LDL-OA (0-200 μM). Cell viability was determined by MTS assay normalized to untreated controls cells. Experiments were performed in triplicate wells with three independent runs. Data are expressed as mean \pm SEM.



Supplementary Figure 4. Mode of cell death. Confocal fluorescence microscopy of H4IIE cells following a 48 hours treatment with LDL nanoparticles (40 μ M). The mode of cell death was assessed by staining the cells with propidium iodide to detect necrosis (red), Annexin V-FITC to detect apoptosis (green) and Hoechst 33342 a counter nuclear stain (blue).



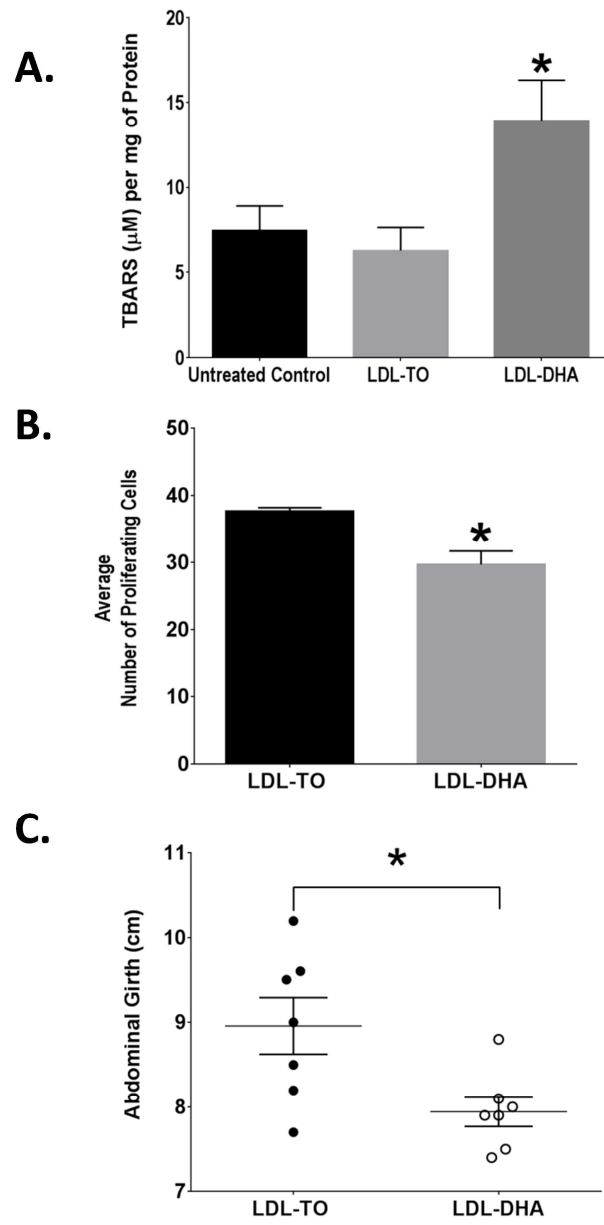
Supplementary Figure 5. Immunohistochemistry of liver and H4IIE tumors after Sham and HAI treatment of LDL nanoparticles (2 mg/kg). Liver and H4IIE tumor tissue samples were collected three days post-treatment. Paraffin-embedded sections of liver and tumor tissue were stained for (A) the proliferation marker Ki-67, (B) the apoptosis marker cleaved caspase-3. Images were taken at 20x magnification. Dotted line indicates liver tumor boundary. Sections in panel B are entirely composed of tumor tissue.



Supplementary Figure 6. Effects of LDL nanoparticle treatment 7 days following HAI.

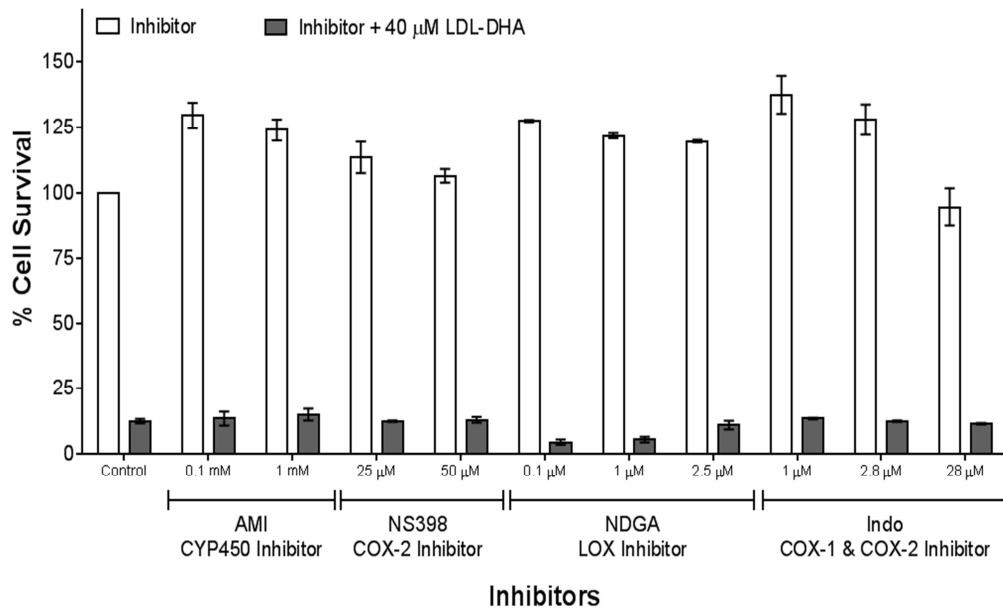
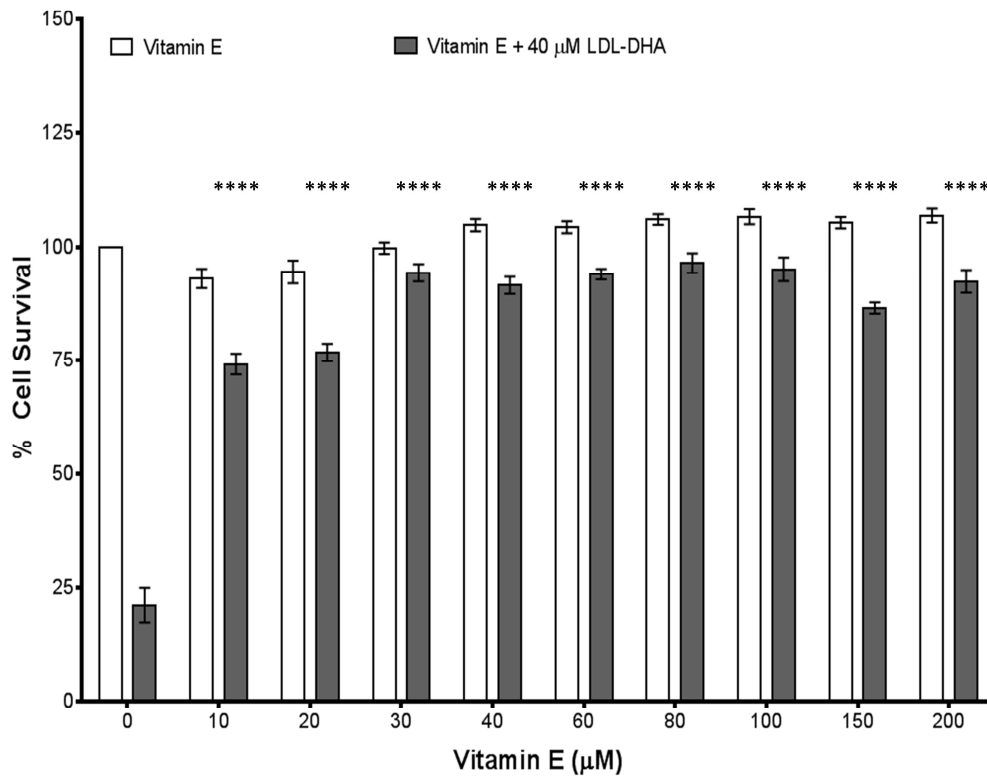
A. *In situ* (top) and excised (bottom) view of liver and H4IIE HCC in a rat orthotopic model of HCC 7 days after hepatic artery injection (HAI) with 2 mg/kg of LDL nanoparticles (n= 3-4 rats per group). Bottom: Ventral view of excised livers with H4IIE HCC (and corresponding histology).

B. Tumor volume 7 days following Sham surgery or LDL nanoparticle HAI. Tumor volume is based on direct size measurements made at the time of sacrifice using the equation $\text{Tumor volume} = \frac{1}{2} (\text{length} \times \text{width}^2)$. Data are expressed as mean \pm SEM. *, $P \leq 0.05$ versus Sham group. $P \leq 0.06$ versus LDL-TO treated group

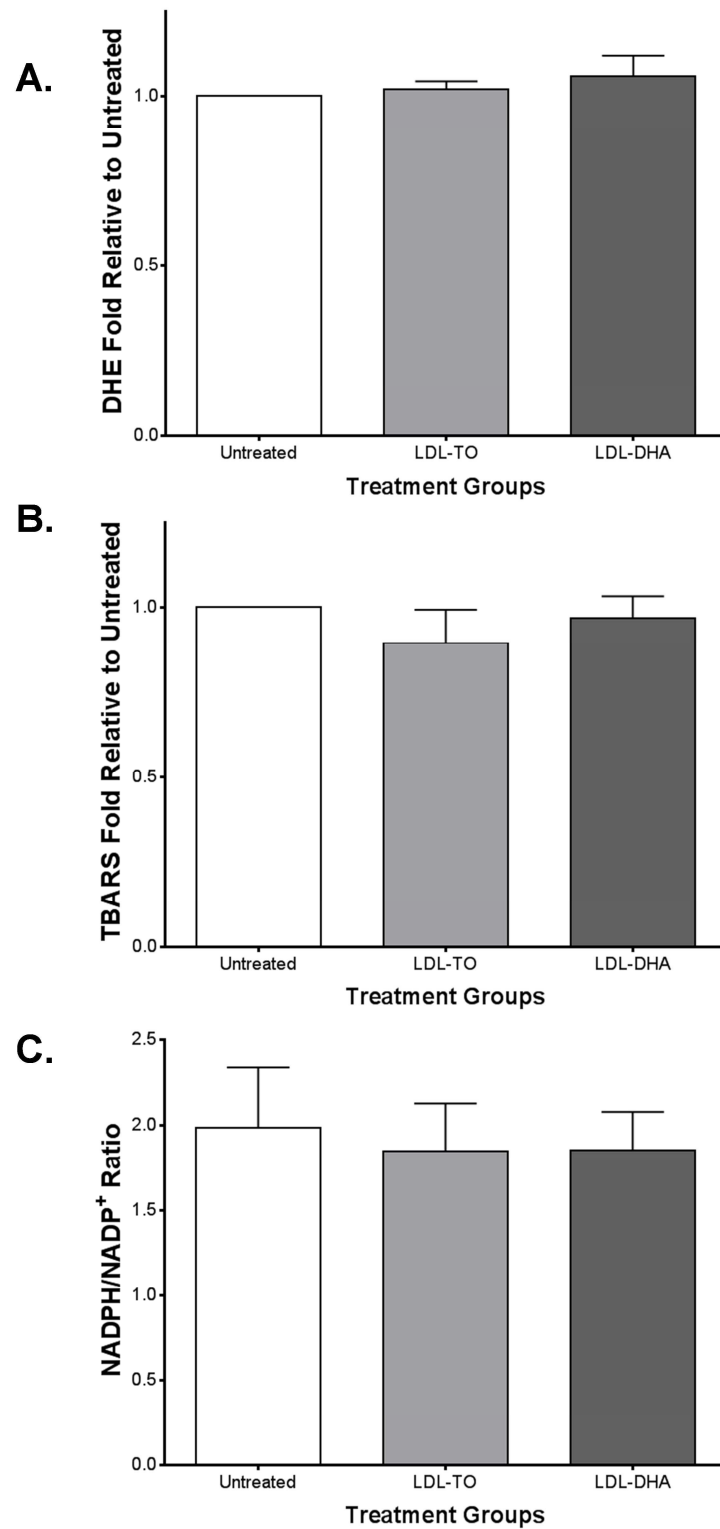


Supplementary Figure 7. Anticancer effects of LDL-DHA in mice with *MYC*-induced HCC.

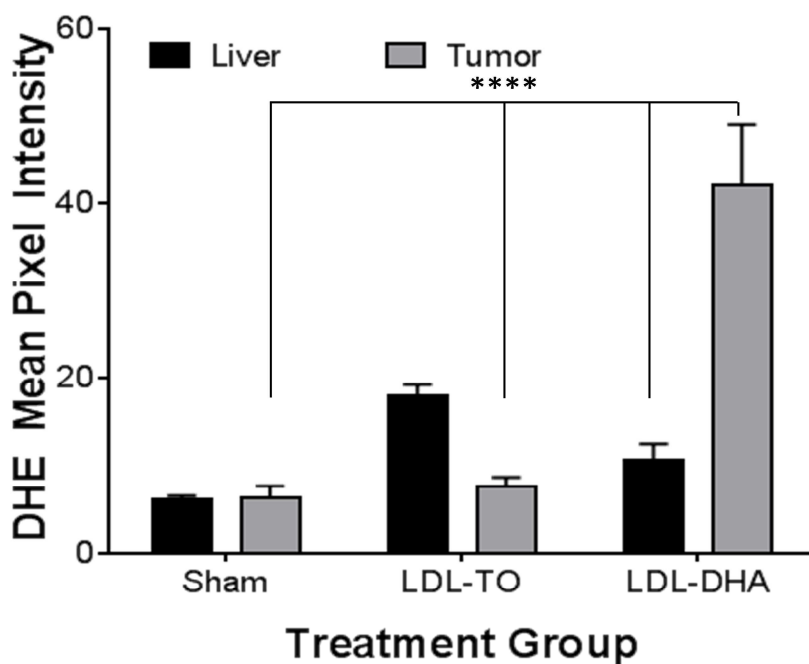
Mice with *MYC*-induced liver cancer received three intravenous treatments of either LDL-TO (n=7) or LDL-DHA (n=7) nanoparticles. The LDL nanoparticles were administered via the tail vein every other day at a dose of 4mg/kg. Twenty four hours after the last dose abdominal girth measurements were performed, animals were euthanized and liver and tumor tissue were collected for subsequent measures of lipid peroxidation (TBARS) and tumor cell proliferation (phosphor-H3). **(A)** The colorimetric TBARS assay was used to measure lipid peroxide levels per mg of tissue in *MYC*-induced mice after LDL nanoparticle treatments. **(B)** Number of Phospho-H3 positive cells per 20x field in the tumors of *MYC*-induced mice following LDL nanoparticle treatments. **(C)** Abdominal girth (circumference in centimeters) of *MYC*-induced mice after LDL nanoparticle treatments. Data are expressed as mean \pm SEM and represent three independent experiments. *, $P \leq 0.05$ versus indicated group.

A.**B.**

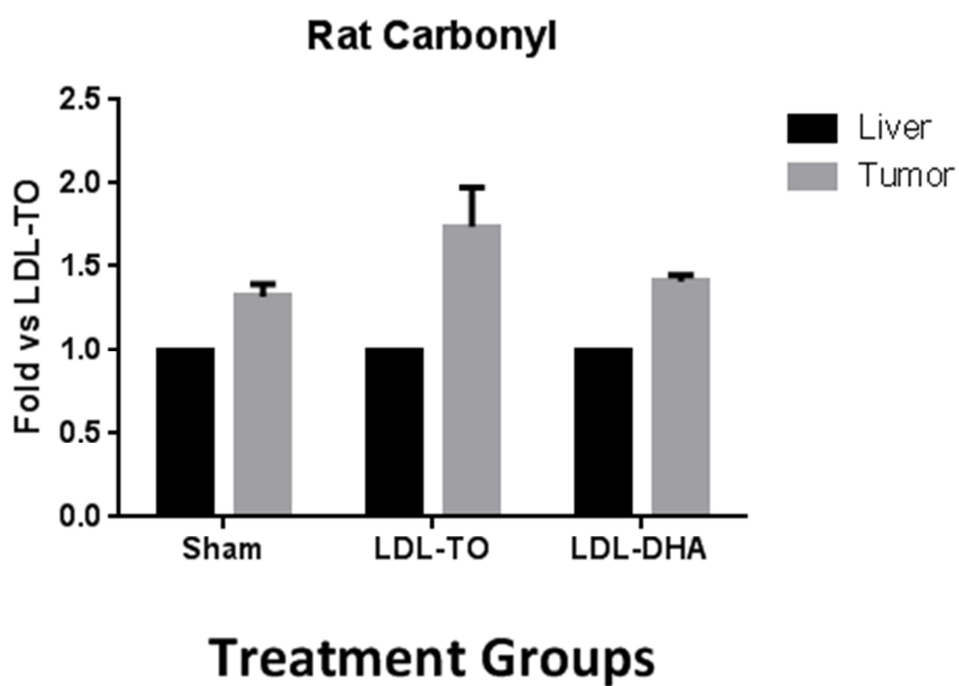
Supplementary Figure 8. Identifying inhibitors of LDL-DHA mediated cytotoxicity. (A) Cell viability assay of H4IIE cells following 72 hours of treatment with 40 μ M LDL-DHA with and without selected concentrations of oxygenase inhibitors: 0.1 mM and 1 mM 1-aminobenzotriazole (AMI) (a CYP450 inhibitor), 25 μ M and 50 μ M NS-398 (a selective inhibitor of cyclooxygenase-2 (COX-2)), 0.1 μ M, 1 μ M and 2.5 μ M Nordihydroguaiaretic acid ((NDGA) a non-selective LOX inhibitor), and 1 μ M, 2.8 μ M and 28 μ M indomethacin (Indo) (a nonselective inhibitor of COX-1 and 2). **(B)** Cell viability assay of H4IIE cells following 72 hours of treatment with Vitamin E (0 - 200 μ M) with or without LDL-DHA (40 μ M). Data are expressed as mean \pm SEM. *, $P \leq 0.05$; **, $P \leq 0.01$; ***, $P \leq 0.001$; ****, $P \leq 0.0001$ versus cells treated only with LDL-DHA.



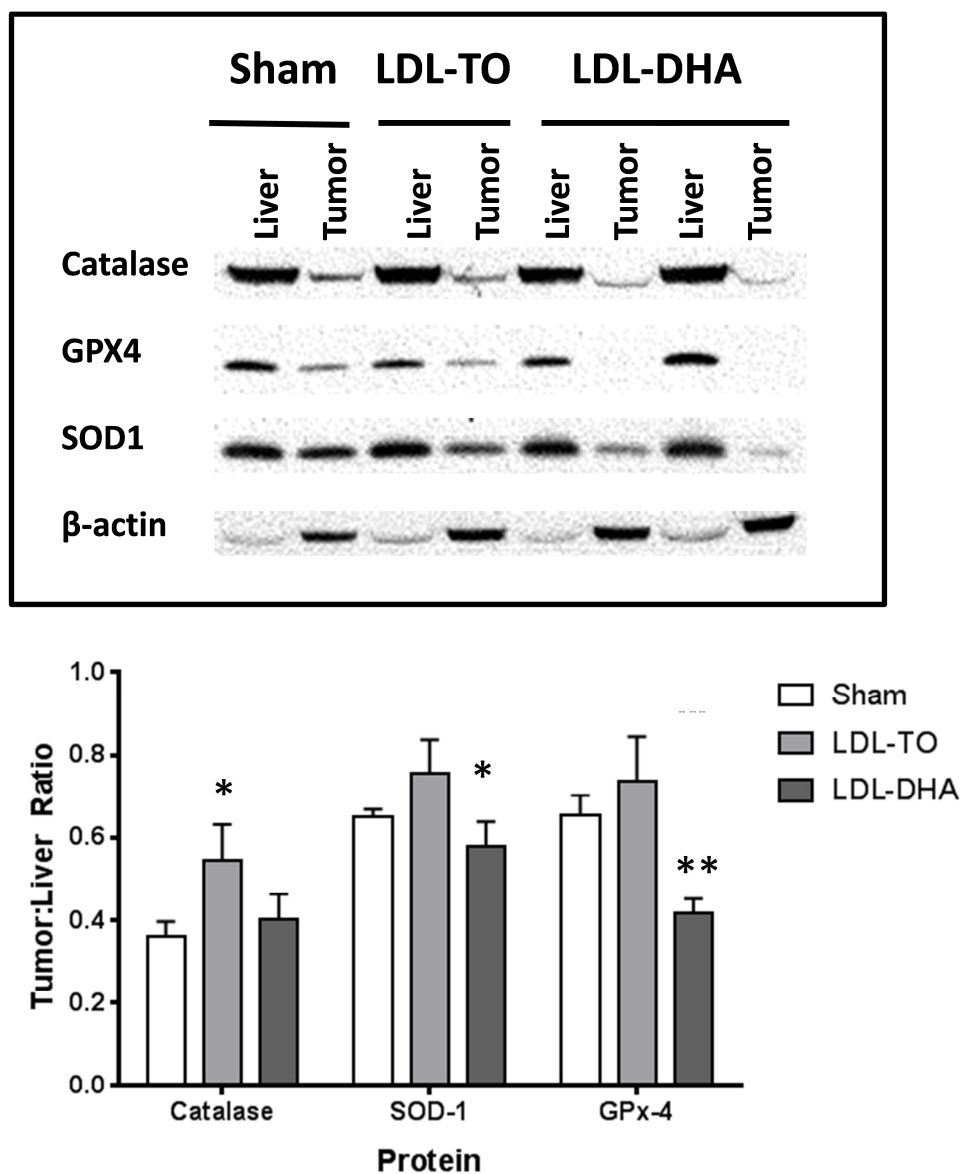
Supplementary Figure 9. *In vitro* measurements of oxidative stress in primary hepatocytes with and without LDL nanoparticle treatment. Six million primary hepatocytes were plated to 100 mm² dishes, serum starved after 24 hours, and then treated for 48 hours with serum free media, 40 μ M LDL-TO, or 40 μ M LDL-DHA. **(A)** Superoxide levels were measured by dihydroethidium fluorescence intensity per mg of cell protein and normalized to the untreated control. **(B)** The colorimetric TBARS assay was used to measure lipid peroxide levels per mg of cell protein and normalized to the untreated control. **(C)** NADPH/NADP⁺ ratio per one million cells was measured by a kinetic colorimetric assay for each treatment group. Data are expressed as mean \pm SEM and represent three independent experiments.



Supplementary Figure 10. Semiquantification of dihydroethidium staining in liver and tumor sections after sham and LDL nanoparticle treatments (2 mg/kg). Liver and H4IIE tumor samples were collected three days post-treatment. Samples were cryoembedded and stained with 2 μ M dihydroethidium for 30 minutes at 37°C. Fluorescence imaging of tissues was performed at 20X with Texas Red filter (λ_{ex} = 596). Images were thresholded to remove background fluorescence and then quantified by calculating mean pixel intensity using ImageJ software; data are presented in mean \pm SEM. *, $P \leq 0.05$; **, $P \leq 0.01$; ***, $P \leq 0.001$; ****, $P \leq 0.0001$ versus indicated groups.



Supplementary Figure 11. Tissue levels of protein carbonyls. Liver and tumor protein carbonyls detected as 2,4-dinitrophenylhydrazine derivatives 72 hours following Sham or HAI LDL nanoparticle treatments (2 mg/kg). Data are expressed as mean \pm SEM relative to Sham liver.



Supplementary Figure 12. Western blot of tissue antioxidants. Protein expression levels of catalase, SOD-1 and GPx-4 in rat liver and H4IIE tumor 7 days after Sham and HAI treatment of LDL nanoparticles (2 mg/kg). Representative blots and quantifications are shown. The data are expressed relative to β -actin expression as a ratio of tumor to liver (mean \pm SEM) for each treatment group. *, $P \leq 0.05$.

Tumor necrosis degree after treatment

Grade	Sham	LDL-TO	LDL-DHA
0	0	0	0
I	1	5	0
II	4	2	2
III	0	0	10

*Apoptotic cells included in necrosis score

Tumor inflammation after treatment

Grade	Sham	LDL-TO	LDL-DHA
0	0	0	0
I	5	5	4
II	0	1	4
III	0	1	4

Supplementary Table 1. Histopathology scores of tumors from Sham and LDL nanoparticle treated rats. Necrosis was graded from 0-3 where: 0= absent; 1= 0-33% necrotic; 2= 34%-66% necrotic; 3= 67%-100% necrotic. Similarly, inflammation was graded on a scale from 0-3 where: 0= absent; 1= minimally affected; 2= mildly affected; 3= moderately affected.

Rat Serum Values	Sham	LDL-TO	LDL-DHA
BUN (mg/dL)	17.2 ± 1.0	13.4 ± 0.9	15.0 ± 1.3
CREA (mg/dL)	0.32 ± 0.03	0.30 ± 0.02	0.28 ± 0.04
ALB (g/dL)	2.6 ± 0.1	2.5 ± 0.1	2.2 ± 0.1
AST (U/L)	141 ± 22	123 ± 5	80 ± 11*
ALT (U/L)	106 ± 13	100 ± 6	72 ± 7*
ALKP (U/L)	100 ± 5	89 ± 4	105 ± 10
TBIL (mg/dL)	0.32 ± 0.05	0.34 ± 0.06	0.30 ± 0.05
GGT (U/L)	<5	<5	<5

Supplementary Table 2. Serum biochemistry of tumor bearing rats 3 days following sham or HAI LDL nanoparticle treatments (2 mg/kg).

Data are expressed as mean ± SEM. *, P ≤ 0.05.

Abbreviations: BUN, blood urea nitrogen; CREA, creatinine; ALB, albumin; AST, aspartate aminotransferase; ALT, alanine aminotransferase; ALKP, alkaline phosphatase; TBIL, total bilirubin; GGT, gamma glutamyltransferase.

Rat Serum Values	Sham	LDL-TO	LDL-DHA
	BUN (mg/dL)	13.7 ± 0.7	13.33 ± 0.07
CREA (mg/dL)	0.35 ± 0.02	0.30 ± 0.00	0.30 ± 0.01
Albumin (g/dL)	2.5 ± 0.1	2.4 ± 0.01	2.4 ± 0.01
AST (U/L)	145.7 ± 9	110.7 ± 23	66.3 ± 3**
ALT (U/L)	102.7 ± 9	81 ± 13	50.7 ± 2**
ALKP (U/L)	124.3 ± 7	131.3 ± 1	150.3 ± 25
TBIL (mg/dL)	0.2 ± 0.00	0.2 ± 0.03	0.2 ± 0.00
GGT (U/L)	<5	<5	<5

Supplementary Table 3. Serum biochemistry of tumor bearing rats 7 days following sham or HAI LDL nanoparticle treatments (2 mg/kg).

Data are expressed as mean ± SEM. *, P ≤ 0.05; **, P ≤ 0.01.

Abbreviations: BUN, blood urea nitrogen; CREA, creatinine; ALB, albumin; AST, aspartate aminotransferase; ALT, alanine aminotransferase; ALKP, alkaline phosphatase; TBIL, total bilirubin; GGT, gamma glutamyltransferase.

References

1. Katsura N, Ikai I, Mitaka T, et al. Long-term culture of primary human hepatocytes with preservation of proliferative capacity and differentiated functions. *J Surg Res* 2002;106:115-23.
2. Li H, Zhang Z, Blessington D, et al. Carbocyanine labeled LDL for optical imaging of tumors. *Acad Radiol* 2004;11:669-77.
3. Beer S, Zetterberg A, Ibric RA, et al. Developmental Context Determines Latency of MYC-Induced Tumorigenesis. *PLoS Biology* 2004;2:e332.
4. Nguyen LH, Robinton DA, Seligson MT, et al. Lin28b is sufficient to drive liver cancer and necessary for its maintenance in murine models. *Cancer Cell* 2014;26:248-61.
5. Erdahl WL, Krebsbach RJ, Pfeiffer DR. A comparison of phospholipid degradation by oxidation and hydrolysis during the mitochondrial permeability transition. *Archives of Biochemistry and Biophysics* 1991;285:252-260.
6. Rahman I, Kode A, Biswas SK. Assay for quantitative determination of glutathione and glutathione disulfide levels using enzymatic recycling method. *Nat Protoc* 2006;1:3159-65.
7. Schafer FQ, Buettner GR. Redox environment of the cell as viewed through the redox state of the glutathione disulfide/glutathione couple. *Free Radical Biology and Medicine* 2001;30:1191-1212.